Journal of Applied Polymer Science

A comparative study on electrosprayed, layer-by-layer, and chemically grafted nanomembranes loaded with iron oxide nanoparticles

Nidia K. Trejo, Margaret Frey
Department of Fiber Science & Apparel Design, Cornell University, Ithaca, New York 14853
Correspondence to: N. K. Trejo (E-mail: nkt23@cornell.edu)

ABSTRACT: In this study, carboxylic acid coated iron oxide nanoparticles (CA-Fe_3O_4 NPs) were applied to Nylon 6 nanomembranes by three different techniques: (1) simultaneous electrospinning/electrospraying, (2) layer-by-layer (LbL) assembly, and (3) chemical grafting. These membranes have potential use toward clean-up of polluted rivers due to the multi-functional properties of the NPs. However, it is critical to evaluate particle retention and stability on fibers to reduce human health and environmental concerns. This study evaluates the NP treatment uniformity, and particle retention of the membranes based on knowledge of the preparation process. Electron microscopy and CIELAB spectrophotometry revealed that the NPs were uniformly dispersed via the electrospun/electrosprayed and grafted methods while non-uniformity was observed on LbL treated membranes. The membranes were washed in solutions of various pH levels (pH = 4, 7, 10) to investigate NP release and retention. Inductively coupled plasma-atomic emission spectroscopy results indicate particle release is driven by pH-dependent, bonding interactions between the NPs and the Nylon 6 fibers. Over 97% of NPs were retained on all treated membranes after washing for 60 min. © 2015 Wiley Periodicals, Inc. J. Appl. Polym. Sci. **2015**, *132*, 42657.

KEYWORDS: electrospinning; fibers; nanoparticles; surfaces and interfaces

Received 1 April 2015; accepted 22 June 2015
DOI: 10.1002/app.42657

INTRODUCTION

For water treatment applications, iron oxide nanoparticles (Fe_3O_4 NPs) have demonstrated high and rapid pick-up rates of pollutants, such as heavy metals and organic dyes from aqueous solutions.[1–6] The adsorption and magnetic properties as well as the high surface to volume ratio of the particles make it an intriguing material for wastewater clean-up. However, the toxicity of free metal oxide nanoparticles on humans and the environment is a subject of ongoing research for scientists who develop the materials and toxicologists.[7–11] By binding the particles to fiber surfaces, many pathways for toxic effects can be eliminated. This study focuses on the preparation processes to develop nanoparticle loaded Nylon 6 membranes, investigating treatment uniformity, and NP retention.

Previously, the release of nanoparticles from commercial textile products was investigated after exposing the materials to different washing conditions, such as tap water/agitation, distilled water/agitation, and traditional laundering.[12–14] In these studies, the details regarding the nanomaterial manufacturing processes were not always available. The focus of these studies was to determine whether NP release was occurring, quantifying, and characterizing the released particles. Knowing the preparation process of NP loading is critical to understand and evaluate the durability on fibrous structures. Therefore, it is important to complete a comprehensive comparative study on the common surface treatments (electrospraying, layer-by-layer assembly, chemical grafting) used for loading NPs on fibrous membranes/fabrics.

Electrospinning is an efficient method to spin continuous, micro- and nano-fibers out of solution. Figure 1 displays the upscaled electrospinning set-up for production of Nylon 6 membranes. When high voltage is applied to the needle filled with polymer solution, the forces of the applied electric field are strong enough to overcome the surface tension of the solution to force it out as a jet. The jet spins toward the grounded collector to form thin, randomly oriented fibers as the solvent evaporates.[15–17] The Nylon 6 polymer was prepared for electrospinning due to its superior tensile strength, abrasion resistance, and stability.[18]

Electrospraying follows a similar concept to electrospinning. When an electric field is applied to the liquid solution, the liquid destabilizes into fines droplets as multiple jets toward the

Additional Supporting Information may be found in the online version of this article.

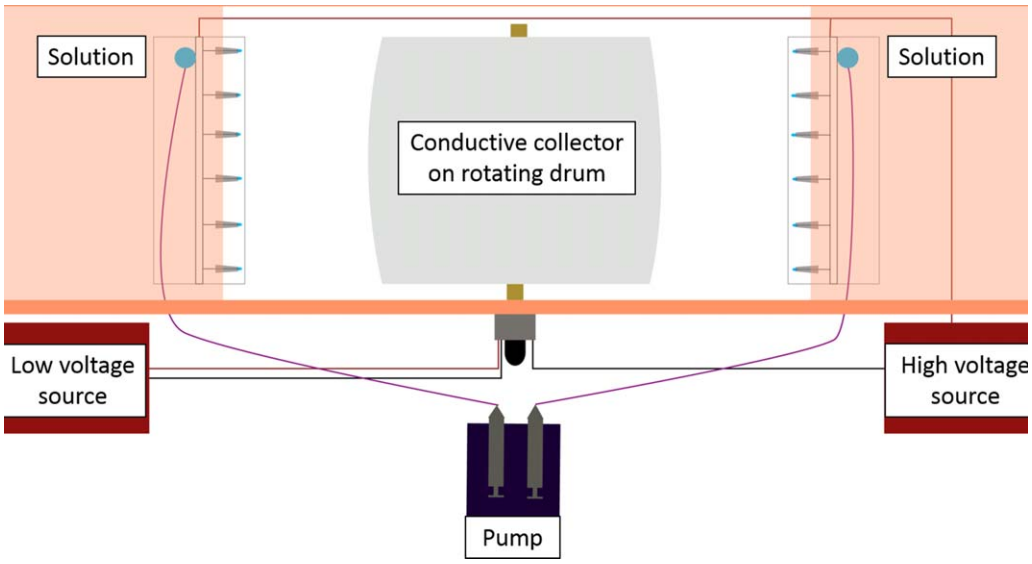

Figure 1. Diagram of upscaled electrospinning set-up (aerial view). [Color figure can be viewed in the online issue, which is available at wileyonlinelibrary.com.]

collector.[19–21] Jaworek *et al.* reported electrospraying various metal oxides on polymeric fibers.[22,23] Electrospraying facilitates uniform NP dispersion within fiber matrices independent of polymer–particle solvent compatibilities and without disrupting homogenous fiber formation.

In layer-by-layer (LbL) assembly, electrostatic interactions form between positively and negatively charged compounds. A charged substrate is immersed into an oppositely charged bath to allow adsorption of the desired compounds. The technique can be repeated to form multiple functional layers.[24–26] Previous reports demonstrate LbL assembly on Nylon 6.[27,28] For example, Dubas *et al.* applied a cationic polyelectrolyte and anionic, poly(methacrylic acid) coated silver NPs on Nylon 6 fabrics.[27]

EDC/NHS chemistry has demonstrated to be a viable method for amidization reactions.[29–32] 1-Ethyl-3-(3-dimethylaminopropyl)carbodiimide (EDC), a coupling agent, activates carboxylate ions to react with primary amines. It is often paired with *N*-hydroxysuccinimide (NHS) to introduce stability to *O*-acylisourea, a key reaction intermediate, by forming an ester group. Previously, several parameters were studied that could lead to successful amide formation. However, discrepancy was observed in the pH environments of the reactions.[30,33,34] For this reason, we explored which pH environment (pH = 4.6 and pH = 8) was suitable for a reaction between the NPs and Nylon 6.

Results of this study are divided into two sections. The first section discusses characterization results for the preparation of the nanomaterials by each method. The second section is a comparative study for treatment uniformity and NP retention/release upon exposure to different pH environments.

EXPERIMENTAL

Materials

Nylon 6 pellets (10 kDa), branched polyethyleneimine (PEI, 50 wt % in H_2O, 750 kDa), 1-ethyl-3-(3-dimethylaminopropyl) carbodiimide hydrochloride (EDC), and sodium phosphate monobasic (NaH_2PO_4) were purchased from Sigma–Aldrich; St. Louis, MO. Sodium hydroxide pellets (NaOH), 88% formic acid, hydrochloric acid (HCl) solution, 69–70% nitric acid, acetone, and methanol were purchased from VWR International, LLC; Radnor, PA. 15 nm sized CA-Fe_3O_4 nanoparticles dispersed in deionized water (5 mg/mL) were supplied by Ocean NanoTech, LLC; Springdale, AR. *N*-Hydroxysulfosuccinimide (sulfo-NHS) was purchased from ProteoChem; Loves Park, IL. The preparation of the buffer solutions is as follows: NaH_2PO_4 was weighed out and dissolved in deionized water for a total concentration of 5 mM. NaOH or HCl was added to adjust the pH of the buffers to pH = 4, 4.6, 5, 6, 7, 8, and 10 before the total volume was reached. These buffers were used for LbL assembly, the grafting reaction, and the washing protocol. Terms referring to pH conditions or buffer solutions in this study refer to the formulation of 5 mM NaH_2PO_4/H_2O + NaOH/HCl.

Preparation of Pristine and Nanoparticle Loaded Membranes Electrospinning. Nylon 6 membranes were produced following previous reports.[35,36] First, 20 wt % Nylon 6 pellets was dissolved in 88% formic acid. The mixture was agitated on a wrist action shaker (Burrell Scientific, Pittsburgh, PA) for 24 h at room temperature to produce a homogeneous polymer solution. The multi-jet needle system surrounded a large rotating drum (6″ × 36″) on each side as shown in Figure 1. A schematic of the needle stand set-up is shown in Supporting Information Figure S1. The polymer solutions were fed to twelve 20 gauge needles (Small Parts, Amazon) at a flow rate of 0.2 mL/h. A 25 kV voltage was applied to the needles. The needle tips were positioned ~10 cm from the grounded drum that was covered with aluminum foil. The electrospinning process was performed at room temperature and a humidity range of 30–40%. Total spinning time for production was 4 h. The system allowed for high production of nanomembranes within a short time period.

Electrospin/Electrospray. For the simultaneous electrospin/electrospray process, one needle stand electrospun fibers while the needle stand on the alternate side electrosprayed the nanoparticle solution. 5 wt % CA-Fe_3O_4 NPs were dispersed in methanol for electrospraying. A 20 wt % Nylon 6 polymer solution was used for electrospinning. The experimental conditions were the same as the electrospinning section with some adjustments. Twenty-five gauge needles and an additional syringe pump was used to feed the NP solution to the needles at a flow rate of 0.2 mL/min. Total operation time of the system was 4.5 h. Simultaneous electrospin/electrospraying was completed in the last 1.5 h. The electrospraying was completed in the last few hours so that the particles would spray on a nanomembrane support as opposed to the aluminum foil collector.

Layer-by-Layer Assembly. Nylon 6 nanomembranes were cut into rectangular samples 5 × ½ $in.^2$ in size. The membranes were dipped in 0.08 wt/wt % PEI and alternatively in 5 wt % CA-Fe_3O_4 NP solution at pH = 7 for 5 min each to produce a total of five bilayers. The samples were rinsed in deionized water between each dip to remove excess and unreacted compounds.

Chemical Grafting with EDC/Sulfo-NHS. EDC (5 mg) and sulfo-NHS (5 mg) were mixed in 1 mL of pH = 4.6 and pH = 8 buffer solutions. They were immediately reacted with 5 mL of 3 wt % CA-Fe_3O_4 NP solution under an inert atmosphere. The mixtures were agitated on a wrist action shaker for 20 min and the Nylon 6 membranes were subsequently immersed in the EDC/sulfo-NHS NP solution for 40 min. The membranes were washed in acetone for 5 h and rinsed lastly in deionized water to remove unbound particles. The reaction worked in a pH = 8 environment, thus those results are discussed in the manuscript.

Quantifying Nanoparticle Load on Membranes and Washing Protocol. The total NP load and amount of NP release were quantified by analyzing the Fe concentration in the samples via inductively coupled plasma-atomic emission spectroscopy (ICP-AES) (Spectro Analytical Instruments). The membranes were dissolved in nitric acid to determine the total NP load applied by each method. For the washing protocol 6–7 mg of membrane from each treatment was immersed in varied pH baths (4, 7, 10). The baths were agitated on a wrist action shaker for 10, 30, and 60 min. Aliquots of 5 mL were taken from each bath to determine the amount of Fe released per allotted time.

CHARACTERIZATION

The morphology of the fibers and nanoparticles was analyzed with electron microscopes (Leica 440-SEM—voltage: 25 kV, WD: 6 mm || LEO-1550-FESEM—voltage: 3–4 kV, WD: 6–7 mm || FEI-T12-TEM-STEM—voltage: 120 kV). For SEM imaging, the nanomembranes were mounted on aluminum stubs (Electron Microscopy Sciences) with carbon tape. Samples were coated with gold–palladium prior to analysis on the Leica 440-SEM for 30 s. A carbon coating was applied to samples analyzed on the LEO-1550-FESEM for 10 s at a power of 25%. For TEM analysis, NP solution droplets were dropped onto a copper grid with a carbon back.

The polymeric coating on the NPs and progress of the grafting reaction was investigated with a Nicolet Magna 560 FTIR spectrometer in attenuated total reflectance mode (ATR-FTIR). The spectra range was 4000–530 cm^{-1} with 64 scans per run, and a resolution of 4 cm^{-1}.

The uniformity of each treatment based on color change was determined using the MacBeth Color Eye 2020+ spectrophotometer. The system analyzes color based on the CIE $L^*a^*b^*$ 3D color coordinates with a standard daylight source D65 and sample area of 1 × 0.5 cm^2. The CIELAB color scale is commonly used in the industries of fiber/textiles, paints, inks, and plastics. It is a quality control measurement for color matching. For textile and fiber analysis it can be useful to very reactions and examine optical effects of treatments.[37–39]

Zeta potential measurements were performed to develop the optimal conditions for the LbL treatment. CA-Fe_3O_4 NP and PEI solutions were evaluated at room temperature from pH = 5 to pH = 8 using the Malvern Nano ZS zetasizer. The solutions filled a disposable folded capillary cell (DTS1060) and buffer solutions were the dispersant for all samples.

RESULTS AND DISCUSSION

Fiber and Nanoparticle Characterization

Morphology of Nanostructures. Figure 2(A) shows a SEM image of 20 wt % Nylon 6 with smooth, round, uniform fibers and an average fiber diameter of ~150 ± 5 nm. Spider-like, nanonet networks appear throughout the morphology of the membranes. Nanonet formation is attributed to phase separation of the charged polymer droplets,[36] the simultaneous binding and intertwining of smaller jets within the dominant whipping jet during electrospinning,[40] and intermolecular hydrogen bonding between protonated —NH_2 and C═O groups in Nylon 6 nanonets and fibers.[41,42] The low boiling point and high dielectric constant properties of formic acid also produce a solvent/polymer mixture susceptible to fine nanonet formation during electrospinning.[43]

Figure 2(B) displays the TEM image of pristine CA-Fe_3O_4 NPs. The particles are colloidal in shape with high monodispersity. The average particle sizes were 15.18 ± 0.95 nm from a sample size of 200.

FTIR of CA-Fe_3O_4 Nanoparticles. FTIR analysis confirms the presence of carboxylic acid functional groups on the NPs as shown in Figure 3. Ocean Nanotech LLC specified that the NPs have an oleic acid capping group and a —COOH polymeric coating. The sample displays transmittance in the regions: 3380, 2920, 2850, 1690, 1540, 1400, and 575 cm^{-1}. The broad IR band at 3380 cm^{-1} is attributed to —OH stretching from the organic coatings and the Fe particles. Sharp alkyl C—H stretches (sp^3) appear at 2920 and 2850 cm^{-1} from the organic layers.[44] The peak at 1690 cm^{-1} corresponds to the carboxylic acid carbonyl stretch from the polymeric coating on the particles. Carbonyl stretches from carboxylic acids are usually observed between 1700 and 1725 cm^{-1}; however, a shift toward a lower

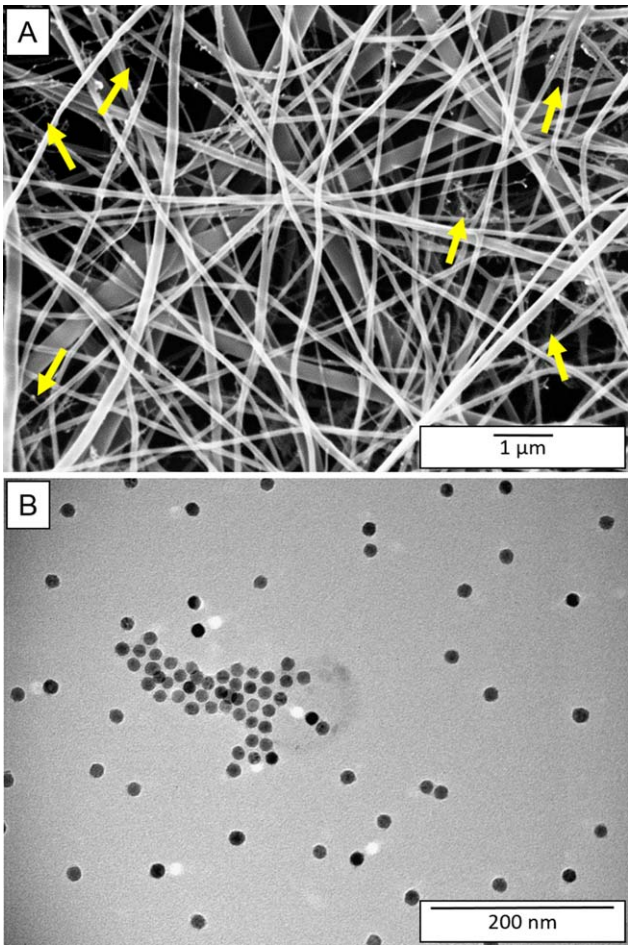

Figure 2. (A) SEM image of pristine 20 wt % Nylon 6 (arrows point to nanonet regions) (B) TEM image of raw CA-Fe_3O_4 nanoparticles. [Color figure can be viewed in the online issue, which is available at wileyonlinelibrary.com.]

wavenumber indicates chemical bonding between the nanoparticle surface and the organic layers.[45,46] Asymmetric and symmetric stretching vibrations of COO^- are apparent at

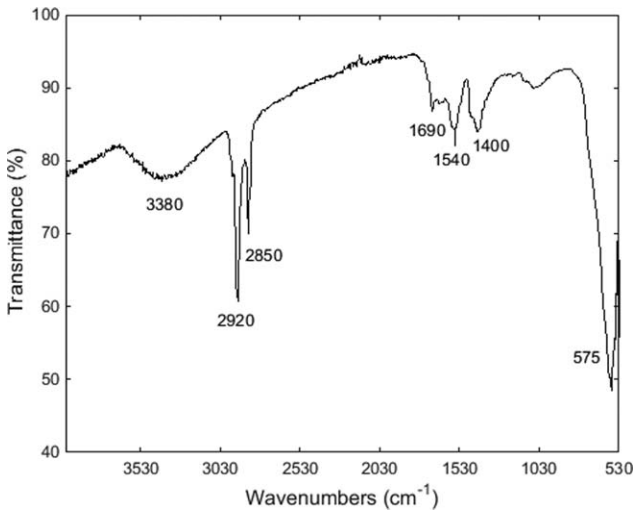

Figure 3. ATR-FTIR spectra of raw CA-Fe_3O_4 nanoparticles.

Figure 4. Initial characterization of electrospray method. Photograph of solvent dispersion on Nylon 6 membranes with multi-jet spraying set-up. The drum collector was stationary and electrospraying occurred for 10 s. [Color figure can be viewed in the online issue, which is available at wileyonlinelibrary.com.]

1400 cm^{-1} and 1540 cm^{-1}, respectively.[47] Metal–oxygen vibrations are common in the fingerprint region. The sharp band at 575 cm^{-1} corresponds to Fe—O stretching at the tetrahedral sites of Fe cations.[48,49]

Results for Optimizing Experimental Conditions

Optimization of Electrospraying. The flow rate of the solution, solvent selection, and droplet dispersion were key parameters to optimize the electrospraying process. The flow rate was optimized to increase spray time and allow for a consistent flow of the solution (0.08–1 mL/min in 0.2 increments). Methanol and acetone were volatile solvents considered for electrospraying due to the rapid evaporation rates.[22] The proper jet bending instability for homogeneous droplet dispersion was introduced by methanol. It has a higher dielectric constant (ε) than acetone. It introduces more free charge and higher surface charge repulsion for jet instability ($\varepsilon_{methanol@20°C} = 32.6$, $\varepsilon_{acetone@20°C} = 20.6$).[50,51] Droplet dispersion was monitored by visual observation. Figure 4 illustrates the droplet dispersion. Methanol was doped with food colorant and dispersion was observed on the collector at varied flow rates with an applied voltage of 25 kV. This route is a simple, low-cost approach to optimize electrospray conditions and directly monitor droplet dispersion on large, mobile collectors. Supporting

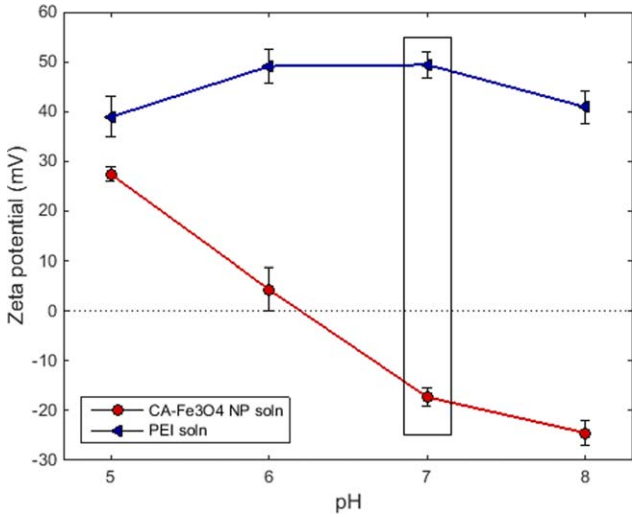

Figure 5. Initial characterization of layer-by-layer method. Zeta potential of CA-Fe_3O_4 nanoparticles and PEI solutions at various pH ranges. [Color figure can be viewed in the online issue, which is available at wileyonlinelibrary.com.]

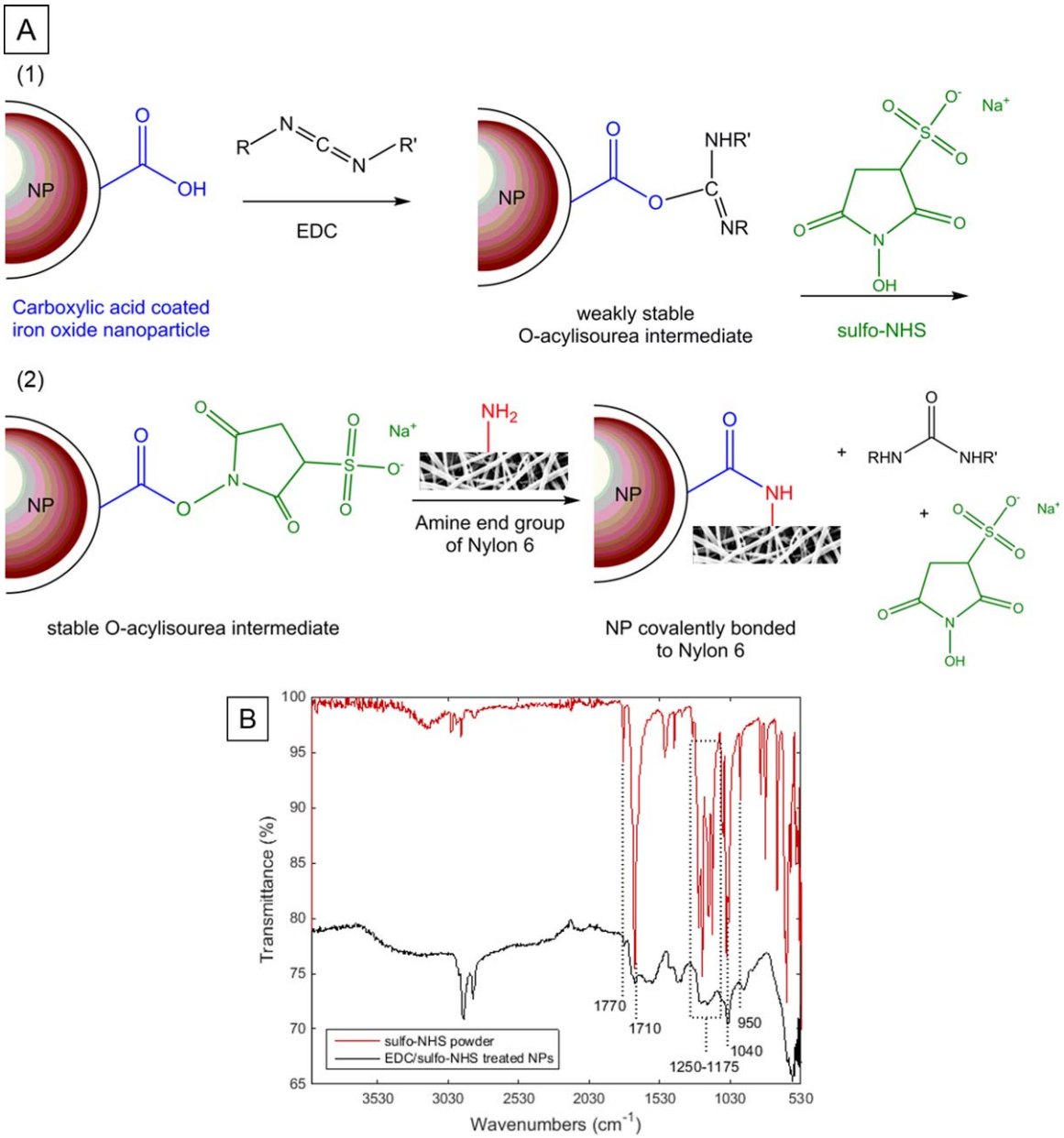

Figure 6. Initial characterization of grafting reaction. (A) Amidization scheme using EDC/sulfo-NHS chemistry. (B) ATR-FTIR spectra of sulfo-NHS powder and EDC/sulfo-NHS treated NPs (pH = 8 environment) prior to reacting with nanomembrane. [Color figure can be viewed in the online issue, which is available at wileyonlinelibrary.com.]

Information Figure S2 shows photographs of the CA-Fe_3O_4 NPs droplets dispersed along the rotating collector.

Optimization of Layer-by-Layer Assembly. Figure 5 depicts the zeta potential measurements of CA-Fe_3O_4 NPs and PEI to determine the optimal pH conditions for alternating surface charges. As the pH increases from pH = 5 to pH = 8 the protonated carboxylic groups on the NPs dissociate to form carboxylate ions. At pH $\geq$ 7 a negative electric potential forms on the NP surfaces. PEI has a positive electric potential within all pH ranges evaluated. The cationic polymer maintains electrostatic stability.[52] Thus, the desired alternating charge in the LbL assembly baths can occur at pH = 7.

Optimization of the Grafting Reaction. Figure 6(A) illustrates a nucleophilic substitution reaction scheme between the NP and Nylon 6. Briefly, the carboxylate ion on a NP reacts with the electron deficient carbon of EDC to form the *O*-acylisourea intermediate. Sulfo-NHS is used as an additional coupling agent because it hydrolyses more slowly in water compared to EDC and helps form a more stable intermediate (1). The nucleophilic —NH_2 groups of Nylon 6 reacts with

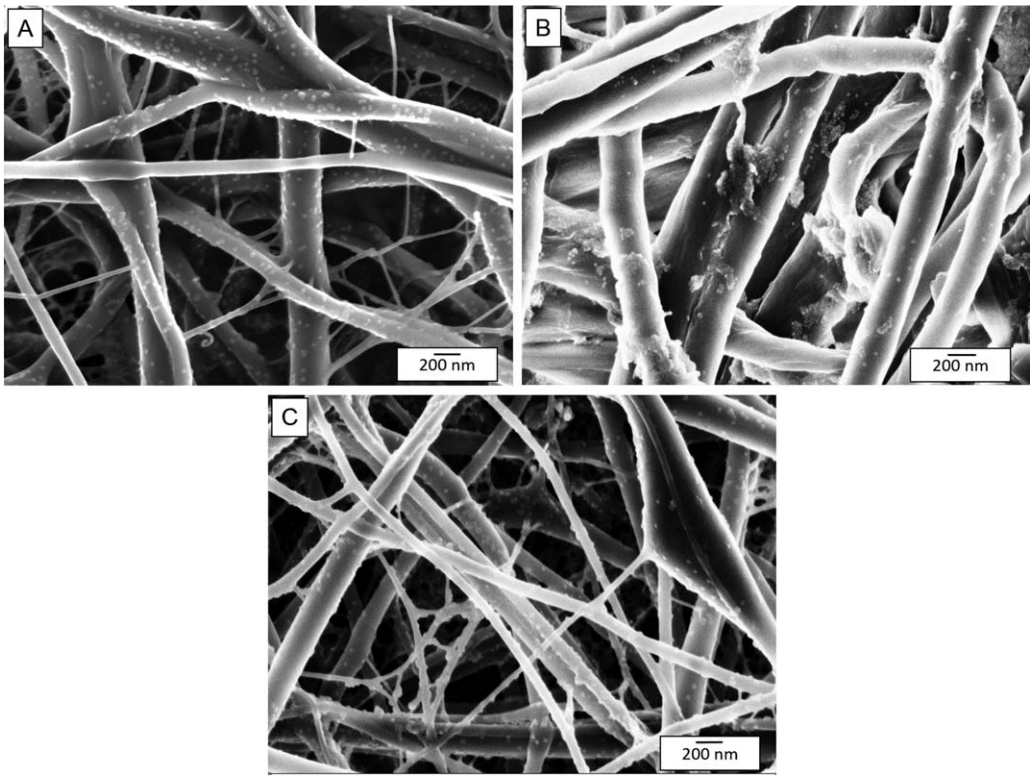

Figure 7. Comparison of FE-SEM images (A) simultaneous electrospin/electrospray, (B) layer-by-layer assembly, and (C) chemical grafting.

the carbonyl carbon center of the intermediate to form the amide bond (2).[30]

Figure 6(B) shows the FTIR spectra of pristine sulfo-NHS powder and EDC/sulfo-NHS treated NPs at pH = 8. Refer to Figure 3 to compare the treated NPs with the raw NPs. Analysis of the spectras in Figure 6(B) confirms the presence of sulfo-NHS on the surface of the NPs as the stable *O*-acylisourea intermediate. New peaks on the NPs from sulfo-NHS are consistent with a previously observed spectra of the coupling agent.[53] The carbonyl stretch from sulfo-NHS appears on the NPs at 1710 cm^{-1}. The new peak at 1770 cm^{-1} is attributed to sulfo-NHS. Bands within the 1250–1175 cm^{-1} range correspond to the sulfonyl (—S═O) stretch, and the peak at 950 cm^{-1} is from the —S—O stretch. The 1040 cm^{-1} peak corresponds to the tertiary amide band of sulfo-NHS. The sample also displays transmittance bands corresponding to prominent NP peaks discussed earlier (3380, 2920, 2850, and 575 cm^{-1}).

The spectra of the treated NPs were also compared to pristine EDC powder; however, no distinguishable peaks were observed belonging to EDC (Supporting Information Figure S3). The FTIR spectra of the reaction between the coupling agents and the NPs at pH = 4.6 is available in Supporting Information Figure S4. Further discussion of these spectras can be found in Supporting Information.

Comparative Results

Nanocomposite Morphology. Figure 7 displays the morphological dispersion of the NPs on nanofibers treated via the electrospun/electrosprayed, LbL, and grafted methods. The fiber diameters did not change and the nanonets are apparent on the membranes treated via the electrospin/electrospray and grafted methods [Figure 7(A,C)]. These membranes show uniform dispersion of the NPs as single particles are observed along the length of the fibers. On the contrary, the LbL treated membranes display fiber swelling and non-uniform NP dispersion [Figure 7(B)]. The PEI coating contributes to fiber swelling and a non-smooth appearance along the fiber surfaces, which is commonly observed on polyelectrolyte coated fibers.[28,54,55] The NPs aggregate in certain regions as clusters while other regions had no observable NPs.

Non-uniformity of the LbL treatment is attributed to the surface charge on the Nylon 6 membrane, the use of colloidal NPs, and bilayer growth kinetics. Although the charge reversal of the compounds was optimized, the Nylon 6 membrane had zwitterionic character at pH = 7. The membrane was neutral, which contributed to irregular adsorption.[27,56] The growth kinetics and uniformity of LbL treatments can also be significantly affected by the NP size (<80 nm). High and rapid affinity of polyelectrolytes occurs toward NPs of smaller size.[57,58] Additionally, during application of the first bilayer the compounds did not have sufficient time to distribute uniformly along the membranes leading to non-uniformity shown in UV–Vis results, Supporting Information Figure S5. The growth of the five bilayers was exponential and occurred the most rapid during application of the first bilayer of the five.

Treatment Uniformity at the Macroscale. CIELAB values for the electrosprayed, LbL, and chemically grafted membranes are displayed in Table I. In column 1, the names of the samples treated by each method and pristine Nylon 6 sample are listed.

Table I. Comparison of ΔL^*, Δa^*, Δb^* Color Coordinate Values of Membranes Treated via Electrospraying, LbL, and Chemical Grafting

Treatment	Sample	L^*	a^*	b^*	ΔL^*	SD	Δa^*	SD	Δb^*	SD
Pristine NY6	Area I	96.58	−0.25	−0.09	n/a	-	n/a	-	n/a	-
Electrosprayed	Area I	90.32	−0.08	8.80	−6.26	± 0.22	0.17	± 0.08	8.89	± 0.53
membranes	Area II	90.76	−0.24	7.76	−5.83		0.01		7.85	
	Area III	90.65	−0.22	8.08	−5.93		0.03		8.17	
LbL	PEI/NY6	94.56	−0.29	0.13	−2.02	-	−0.04	-	0.22	-
membranes	Area I	91.30	0.33	4.31	−5.28	± 1.78	0.58	± 0.59	4.40	± 2.88
	Area II	88.91	0.91	6.10	−7.67		1.16		6.19	
	Area III	87.83	1.51	9.94	−8.75		1.76		10.03	
Grafted	Area I	90.67	−0.14	7.24	−5.91	± 0.60	0.11	± 0.64	7.33	± 0.64
membranes	Area II	89.48	1.05	8.45	−7.10		1.30		8.54	
	Area III	90.16	0.05	7.47	−6.42		0.30		7.56	

Column 2 displays the samples evaluated in three different areas. The L^*, a^*, and b^* columns are raw values of the color coordinates. L^* values range from 0 (black) to 100 (white) representing the lightness and darkness of a material. The a^* axis represents the color red in the positive direction, and green in the negative direction. The b^* axis represents yellow in the positive direction, and blue in the negative direction. The ΔL^*, Δa^*, and Δb^* columns are values obtained from the calculation in eq. (1) and standard deviations of the three areas examined are listed beside these columns.

$$L^*_{\text{treated}} - L^*_{\text{pristine}} = \Delta L^*. \quad (1)$$

The color change observed is similar on all treated membranes. ΔL^* are negative values, Δa^* are positive, and Δb^* are positive. The samples darkened, got slightly reddish, and more yellow corresponding to the inherent tan color of the NP solutions.

The membranes treated via the electrospray and grafted methods display uniform NP dispersion in the three areas examined. The standard deviation between ΔL^*, Δa^*, and Δb^* values of electrospun/electrosprayed and grafted samples are less than ± 1.

CIELAB values for the LbL membranes reveal non-uniformity of the treatment. The standard deviation of ΔL^*, Δa^*, and Δb^* values are ± 1.78, ± 0.59, and ± 2.88, respectively. In comparison to pristine Nylon 6, the pure PEI polymer introduced a slightly darker, greener, and yellower color on the membrane. It is important to evaluate treatment uniformity for fiber preparation processes because the uniformity can affect end performance.[27] The CIELAB results coincide with conclusions made from the SEM images.

Total CA-Fe_3O_4 NP Loads on Nylon-6 Membranes. The average total Fe was 7.74 ± 0.28 ppm, 3.10 ± 0.18 ppm, and 18.08 ± 1.75 ppm, for the electrospun/electrosprayed, LbL, and grafted membranes, respectively. The membranes treated via the grafting method contain the highest NP load, followed by the electrospray and LbL treated membranes.

Post-Washing Results: Nanoparticle Retention and Release. Molecular forces between the NPs and Nylon 6 by the three treatment methods includes covalent bonding, hydrogen bonding, ionic bonding, dipole–dipole, and van der Waals forces. Hydrogen bonding is the dominant force between electrosprayed NPs and the electrospun membranes. Ionic bonding is the main interaction holding the LbL network together. For the grafting reaction, covalent bonding is the major binding force. Dipole–dipole and van der Waals forces are present on all treated membranes. These molecular forces are important to acknowledge in analyzing particle retention/release in the varied pH environments. With exposure to varied pH environments, the dominant interactions between the NPs and Nylon 6 are ionic or electrostatic interactions.

Some NP release was observed by all three treatments methods after exposure to the various pH levels. The release is driven by molecular bonding interactions, the pH environment, and surface charges on the materials.[59] The NP–Nylon 6 bonding interactions and release behavior is supported by the zeta potential results and the ability of Nylon 6 to selectively charge. The Nylon 6 polymer contains —NH_2 and —COOH groups that can introduce an overall positive or negative charge on the fiber surface based on the pH environment.[56,60] The percent of Fe released after washing was calculated using eq. (2):

$$\%\ \text{of Fe released} = \left[\frac{\text{Fe released}}{\text{Fe total}}\right] \times 100. \quad (2)$$

Figure 8(A) displays the amount of Fe released from electrospun/electrosprayed membranes. At 60 min, the lowest percent of Fe release, 0.17%, occurred at pH = 4 while higher percent of Fe release, 0.77%, was observed at pH = 7 and pH = 10. The NPs have high retention at low pH due to hydrogen bond attractions to the fibers. At low pH, the carboxyl groups on NPs are protonated and gain affinity to the Nylon 6 membrane because the amine and carboxyl groups along the polymer chains also become protonated. At pH $\geq$ 7 the protons on carboxyl groups of the NPs dissociate. Proton dissociation also occurs for the functional groups on Nylon 6 to form an overall negative surface charge and electrostatic repulsion to initiate NP release overtime.

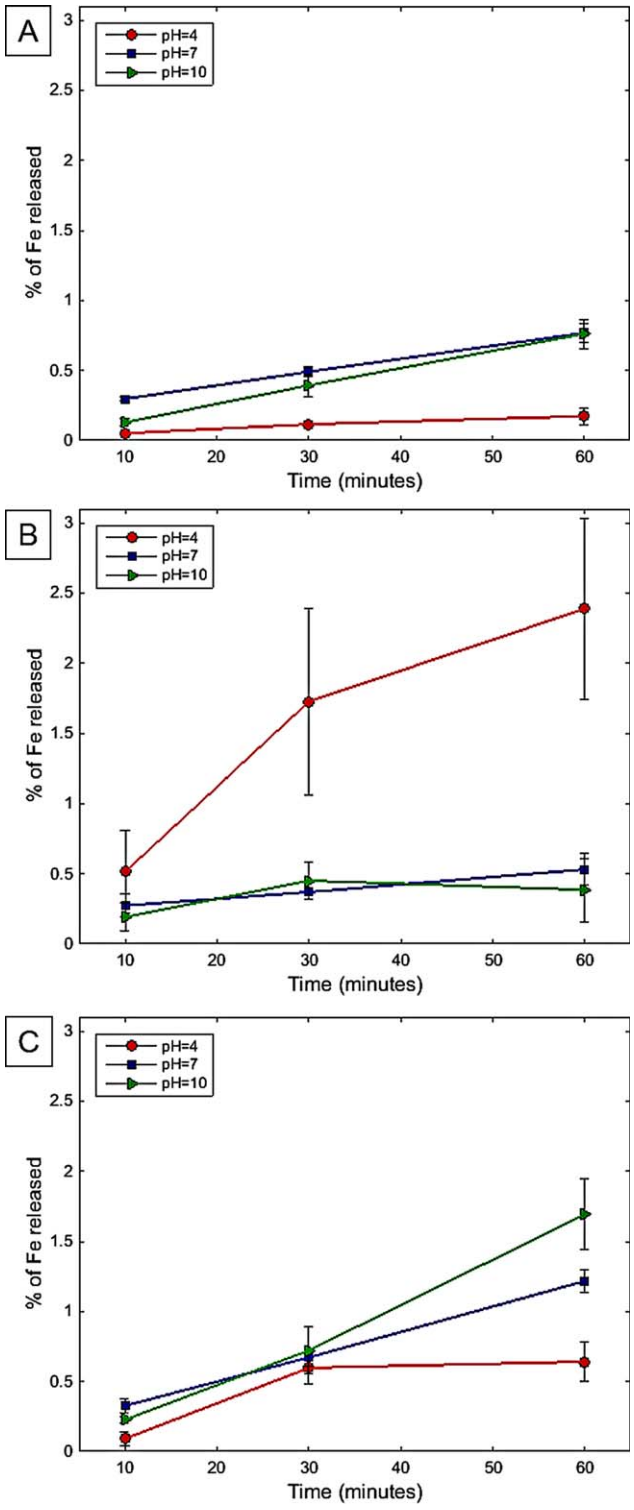

Figure 8. Percent of Fe released from (A) electrospun/electrosprayed, (B) LbL treated, and (C) grafted membranes washed in varied pH baths. [Color figure can be viewed in the online issue, which is available at wileyonlinelibrary.com.]

Figure 8(B) displays the ICP-AES results from the LbL treated membranes. By 60 min, results reveal low % of Fe release with 0.53% at pH = 7 and 0.39% at pH = 10. At pH = 4, the percent of Fe released into the bath increases to a maximum of 2.39% at 60 min. In this case, high NP retention is observed at high pH levels because of strong electrostatic forces between the Nylon 6 fibers, PEI, and the NPs. In a high pH environment, Nylon 6 has an overall negative surface charge, PEI remains positively charged, and carboxylate ions form on the surface of the NPs throughout the bilayers to keep the bonding network electrostatically stable. At low pH, Nylon 6 becomes positively charged while the PEI remains positive and carboxyl groups on the NPs protonate. The lack of adequate electrostatic interactions at low pH initiates repulsion between the compounds and higher NP release into the bath. Large standard errors are observed at low pH from the instability and non-uniformity of the five bilayers applied to the membranes.

Figure 8(C) displays the percent Fe released from the grafted membranes. Although the preparation process for the grafted membranes was optimized to minimize unbound NPs on the fiber surfaces and covalent bonding was the major binding force, excess NPs are still present indicated by the NP release results. At 60 min, a high percent of Fe release is observed at pH $\geq$ 7 similar to the electrosprayed membranes. 1.22% of Fe released at pH = 7 and 1.69% of Fe released at pH = 10 while lower release, 0.64%, occurred at pH = 4. At low pH, the non-bonded NPs have affinity to the Nylon 6 membranes due to electrostatic attraction and hydrogen bonding occurring between the sulfo-NHS ester activated NPs and the protonated carboxyl groups on Nylon 6. At high pH, NP release is noted due to electrostatic repulsion between the $-SO_3^-$ groups on the ester activated NPs and the carboxylate ions on Nylon 6.

NPs incorporated via the electrospray and grafting method released the least NPs at low pH while the LbL method had the lowest particle release under neutral and high pH conditions. At the highest NP release conditions the electrospun/electrosprayed membranes retained 99.2% of the particles, the LbL membranes retained 97.6%, and the grafted membranes retained 98.3%, respectively. Overall, the lowest NP release was observed with the electrosprayed membranes because the NPs became physically entrapped between the fibrous network. The NPs applied by the LbL and grafting treatments are susceptible to coming off more easily because the particles are applied as surface treatments on the membranes. These results support Geranio *et al.*'s work in that chemically bonded and surface coating treatments of NPs on fibers are more likely to release particles compared to NPs incorporated onto fibers with binders or directly inside the fiber.[14] Additionally, it is important to note that agitation was a contributing factor in particle release, and release was independent from total NP loadings.[13]

This research simply addresses pH level as a water chemistry parameter. We acknowledge that nanoparticle durability on membranes can be affected by other water chemistry variables, such as buffering capacity, hardness, salinity, and natural organic matter.[61,62] Further research is needed to investigate the effect of other water variables on unintended NP release from nanomembranes.

CONCLUSIONS

In comparing the three preparation methods, the electrospun/electrosprayed and grafting methods allowed for good NP

dispersion and uniformity on the fibrous membranes. LbL assembly could not provide uniform NP distribution. ICP-AES studies confirm that the preparation process and bonding interactions control the durability of the nanoparticles on fibrous membranes. Results showed low NP release from all three methods based on a combination of electrostatic and intermolecular forces between the treated membranes and pH environment. This study can be useful to consider how the preparation process of NP loaded membranes and fabrics can inform NP durability when the material is exposed to different conditions during its life use in application.

ACKNOWLEDGMENTS

Special thanks to Lara Estroff (MSE), Xia Zeng (FSAD), John Hunt (CCMR), John Grazul (CCMR), Malcolm Thomas (CCMR), and Catherine Reyes (FSAD). This work made use of the Cornell Center for Materials Research Shared Facilities which are supported through the NSF MRSEC program (DMR-1120296). Additional facilities we would like to acknowledge are the Nanobiotechnology Center (NBTC) and the Cornell Nutrient Analysis Laboratory (CNAL).

REFERENCES

1. Si, Y.; Ren, T.; Ding, B.; Yu, J.; Sun, G. *J. Mater. Chem.* **2012**, *22*, 4619.
2. Zeng, G.; Pang, Y.; Zeng, Z.; Tang, L.; Zhang, Y.; Liu, Y.; Zhang, J.; Lei, X.; Li, Z.; Xiong, Y.; Xie, G. *Langmuir* **2011**, *28*, 468.
3. Shin, S.; Jang, J. *Chem. Commun.* **2007**, 4230.
4. Guo, L.; Li, J.; Zhang, L.; Li, J.; Li, Y.; Yu, C.; Shi, J.; Ruan, M.; Feng, J. *J. Mater. Chem.* **2008**, *18*, 2733.
5. Zhang, W.; Shi, X.; Zhang, Y.; Gu, W.; Li, B.; Xian, Y. *J. Mater. Chem. A* **2013**, *1*, 1745.
6. Liu, J.; Du, X. *J. Mater. Chem.* **2011**, *21*, 6981.
7. Davis, J. M.; Long, T. C.; Shatkin, J. A.; Wang, A. U.S. Environmental Protection Agency; U.S. Environmental Protection Agency: Washington, DC, **2010**.
8. Cañas-Carrell, J. E.; Li, S.; Parra, A. M.; Shrestha, B.; Njuguna, J.; Pielichowski, K.; Zhu, H. "In 10 - Metal oxide nanomaterials: health and environmental effects," *Health and Environmental Safety of Nanomaterials*; Woodhead Publishing: **2014**, p 200–221. http://www.sciencedirect.com/science/article/pii/B9780857096555500106
9. Silva, T.; Pokhrel, L. R.; Dubey, B.; Tolaymat, T. M.; Maier, K. J.; Liu, X. *Sci. Total Environ.* **2014**, *468–469*, 968.
10. Anastas, P. T.; Warner, J. C. Green Chemistry: Theory and Practice; Oxford University Press, **2000**, 152.
11. Nowack, B.; Ranville, J. F.; Diamond, S.; Gallego-Urrea, J. A.; Metcalfe, C.; Rose, J.; Horne, N.; Koelmans, A. A.; Klaine, S. J. *Environ. Toxicol. Chem.* **2012**, *31*, 50.
12. Benn, T.; Cavanagh, B.; Hristovski, K.; Posner, J. D.; Westerhoff, P. *J. Environ. Qual.* **2010**, *39*, 1875.
13. Benn, T. M.; Westerhoff, P. *Environ. Sci. Technol.* **2008**, *42*, 4133.
14. Geranio, L.; Heuberger, M.; Nowack, B. *Environ. Sci. Technol.* **2009**, *43*, 8113.
15. Darrell, H. R. A. I. C. *Nanotechnology* **1996**, *7*, 216.
16. Reneker, D. H.; Yarin, A. L. *Polymer* **2008**, *49*, 2387.
17. Li, D.; Xia, Y. *Adv. Mater.* **2004**, *16*, 1151.
18. Domininghaus, H. *Plastics for Engineers: Materials, Properties, Applications*; Hanser Gardner Publishers: Munich, New York, January **1993**, p 785.
19. Cloupeau, M.; Prunet-Foch, B. *J. Electrostat.* **1990**, *25*, 165.
20. Rayleigh, L. *Philos. Mag. Ser.* **1882**, *5*, 184.
21. Salata, O. V. *Curr. Nanosci.* **2005**, *1*, 25.
22. Jaworek, A.; Sobczyk, A. T. *J. Electrostat.* **2008**, *66*, 197.
23. Jaworek, A.; Krupa, A.; Lackowski, M.; Sobczyk, A. T.; Czech, T.; Ramakrishna, S.; Sundarrajan, S.; Pliszka, D. *J. Electrostat.* **2009**, *67*, 435.
24. Ariga, K.; Hill, J. P.; Ji, Q. *Phys. Chem. Chem. Phys.* **2007**, *9*, 2319.
25. Ariga, K.; Yamauchi, Y.; Rydzek, G.; Ji, Q.; Yonamine, Y.; Wu, K. C. W.; Hill, J. P. *Chem. Lett.* **2014**, *43*, 36.
26. Decher, G. In Multilayer Thin Films; Wiley-VCH Verlag GmbH & Co: KGaA, **2003**.
27. Dubas, S. T.; Kumlangdudsana, P.; Potiyaraj, P. *Colloids Surf. A: Physicochem. Eng. Asp.* **2006**, *289*, 105.
28. Park, J. H.; Kim, B. S.; Yoo, Y. C.; Khil, M. S.; Kim, H. Y. *J. Appl. Polym. Sci.* **2008**, *107*, 2211.
29. Pieper, J. S.; Hafmans, T.; Veerkamp, J. H.; van Kuppevelt, T. H. *Biomaterials* **2000**, *21*, 581.
30. Bartczak, D.; Kanaras, A. G. *Langmuir* **2011**, *27*, 10119.
31. Humphrey, J. M.; Chamberlin, A. R. *Chem. Rev.* **1997**, *97*, 2243.
32. Sapsford, K. E.; Algar, W. R.; Berti, L.; Gemmill, K. B.; Casey, B. J.; Oh, E.; Stewart, M. H.; Medintz, I. L. *Chem. Rev.* **2013**, *113*, 1904.
33. Nakajima, N.; Ikada, Y. *Bioconjug. Chem.* **1995**, *6*, 123.
34. Orelma, H.; Filpponen, I.; Johansson, L. S.; Osterberg, M.; Rojas, O. J.; Laine, J., *Biointerphases* **2012**, *7*, 61.
35. Frey, M.; Li, L. *J. Eng. Fibers Fabrics* **2007**, 31.
36. Ding, B.; Li, C.; Miyauchi, Y.; Kuwaki, O.; Seimei, S. *Nanotechnology* **2006**, *17*, 3685.
37. Fairchild, M. D. In Color Appearance Models; John Wiley & Sons, Ltd: **2013**, p 199–212. http://dx.doi.org/10.1002/9781118653128.ch10.
38. Liu, N.; Sun, G.; Gaan, S.; Rupper, P. *J. Appl. Polym. Sci.* **2010**, *116*, 3629.
39. Rahman, M. M.; Ho, K.; Netravali, A. N. *J. Appl. Polym. Sci.* **2015**, *132*, n/a.
40. Tsou, S.-Y.; Lin, H.-S.; Wang, C. *Polymer* **2011**, *52*, 3127.
41. Pant, H. R.; Bajgai, M. P.; Yi, C.; Nirmala, R.; Nam, K. T.; Baek, W.-I.; Kim, H. Y. *Colloids Surf. A: Physicochem. Eng. Asp.* **2010**, *370*, 87.
42. Wang, X.; Ding, B.; Sun, G.; Wang, M.; Yu, J., *Prog. Mater. Sci.* **2013**, *58*, 1173.

43. Andrady, A. L. Science and Technology of Polymer Nanofibers; Wiley: Hoboken, NJ, **2008**.
44. Carmen Bautista, M.; Bomati-Miguel, O.; del Puerto Morales, M.; Serna, C. J.; Veintemillas-Verdaguer, S. *J. Magn. Magn. Mater.* **2005**, *293*, 20.
45. Zhang, D.; Karki, A. B.; Rutman, D.; Young, D. P.; Wang, A.; Cocke, D.; Ho, T. H.; Guo, Z. *Polymer* **2009**, *50*, 4189.
46. Guo, Z.; Henry, L. L.; Palshin, V.; Podlaha, E. J. *J. Mater. Chem.* **2006**, *16*, 1772.
47. Guan, X.-H.; Chen, G.-H.; Shang, C. *J. Environ. Sci.* **2007**, *19*, 438.
48. Waldron, R. D. *Phys. Rev.* **1955**, *99*, 1727.
49. Yu, B. Y.; Kwak, S.-Y. *J. Mater. Chem.* **2010**, *20*, 8320.
50. Sun, Z.; Deitzel, J. M.; Knopf, J.; Chen, X.; Gillespie, J. W. *J. Appl. Polym. Sci.* **2012**, *125*, 2585.
51. Smallwood, I. M. *Handbook of Organic Solvent Properties* Butterworth-Heinemann: Oxford, **1996**, p ix–xxi. http://www.sciencedirect.com/science/article/pii/B9780080523781500049
52. Kim, Y. S.; Davis, R.; Cain, A. A.; Grunlan, J. C. *Polymer* **2011**, *52*, 2847.
53. Erogbogbo, F.; Tien, C.-A.; Chang, C.-W.; Yong, K.-T.; Law, W.-C.; Ding, H.; Roy, I.; Swihart, M. T.; Prasad, P. N. *Bioconjug. Chem.* **2011**, *22*, 1081.
54. Hyde, K.; Rusa, M.; Juan, H. *Nanotechnology* **2005**, *16*, S422.
55. Hyde, G. K.; Park, K. J.; Stewart, S. M.; Hinestroza, J. P.; Parsons, G. N. *Langmuir* **2007**, *23*, 9844.
56. Roberts, G. A. F. *J. Soc. Dyers Colourists* **1996**, *112*, 62.
57. Elbakry, A.; Wurster, E.-C.; Zaky, A.; Liebl, R.; Schindler, E.; Bauer-Kreisel, P.; Blunk, T.; Rachel, R.; Goepferich, A.; Breunig, M. *Small* **2012**, *8*, 3847.
58. Zhou, J.; Pishko, M. V.; Lutkenhaus, J. L. *Langmuir* **2014**, *30*, 5903.
59. Matlock-Colangelo, L.; Cho, D.; Pitner, C. L.; Frey, M. W.; Baeumner, A. J. *Lab on a Chip* **2012**, *12*, 1696.
60. Mathieson, A. R.; Whewell, C. S.; Williams, P. E. *J. Appl. Polym. Sci.* **1964**, *8*, 2009.
61. Pokhrel, L. R.; Dubey, B.; Scheuerman, P. R. *Environ. Sci.: Nano* **2014**, *1*, 45.
62. Sani-Kast, N.; Scheringer, M.; Slomberg, D.; Labille, J.; Praetorius, A.; Ollivier, P.; Hungerbühler, K. *Sci. Total Environ.* http://www.sciencedirect.com/science/article/pii/S0048969714017276